HemaSphere
Powered by EHA

EHA EUROPEAN HEMATOLOGY ASSOCIATION

Letter

OPEN ACCESS

Phosphoproteomic Characterization of Primary AML Samples and Relevance for Response Toward FLT3-inhibitors

David G. J. Cucchi[1], Carolien Van Alphen[1,2,3], Sonja Zweegman[1], Bo Van Kuijk[1], Zinia J. Kwidama[1], Adil al Hinai[4,5], Alexander A. Henneman[2,3], Jaco C. Knol[2,3], Sander R. Piersma[2,3], Thang V. Pham[2,3], Connie R. Jimenez[2,3], Jacqueline Cloos[1], Jeroen J. W. M. Janssen[1]

Correspondence: Jeroen J. W. M. Janssen (j.janssen@amsterdamumc.nl)

Kinase hyperactivity is a common driver of acute myeloid leukemia (AML) and serves as a therapeutic target.[1] The most frequent activating genetic aberrations in AML are internal tandem duplications (~23%) and tyrosine kinase domain mutations (~7%) of FMS-like tyrosine kinase 3 (*FLT3*-ITD and *FLT3*-TKD), and the presence of *FLT3*-ITD negatively affects survival.[2] Combined with chemotherapy, FLT3-Tyrosine Kinase Inhibitor (FLT3-TKI) midostaurin improves overall survival in newly diagnosed *FLT3*-mutated AML, whereas the single agent gilteritinib proved superior to chemotherapy in relapsed/refractory FLT3-mutated AML.[2] The presence of *FLT3*-ITD is predictive for response to FLT3-TKIs,[3] yet 41%–56% of *FLT3*-WT patients respond to *FLT3*-TKIs, indicating alternative possibilities of FLT3 pathway activation or TKI off-target effects leading to unexpected treatment response.[4] Others have identified genomic and global phosphorylation markers associated with FLT3-TKI response in *FLT3*-WT AML.[5,6] As the primary targets of currently approved FLT3-TKIs are tyrosine (Y) kinases, we hypothesized that the direct evaluation of tyrosine kinome could reveal phosphorylation markers associated with FLT3-TKI response. Therefore, we performed both label-free pY-based and global phosphoproteomics[7] in 35 primary AML samples (18 *FLT3*-WT, 17 *FLT3*-ITD, details provided in Supplemental Digital Table 1, http://links.lww.com/HS/A167) to identify differential phosphorylation underlying response to the FLT3-TKIs gilteritinib and midostaurin.

We identified a total of 3.024 unique phosphosites (median 1.666 per sample, range 1.091–2.118; Supplemental Digital Figure 1, http://links.lww.com/HS/A167 and Supplemental Digital Table 2A, http://links.lww.com/HS/A167) in the pY and 27.821 unique phosphosites in the global phosphoproteome dataset. Two samples were excluded due to the low number (382 and 550) of identified phosphosites. Details are provided in the Supplemental Digital Materials and Methods, http://links.lww.com/HS/A167 and Supplemental Digital Table 2B, http://links.lww.com/HS/A167. We then assessed ex vivo response toward FLT3-TKIs by liquid culture and cell viability testing of AML blasts using flow cytometry (Supplemental Digital Figure 2, http://links.lww.com/HS/A167). Of 33, 19 AMLs yielded interpretable dose-response curves and were included in further analyses. As expected, *FLT3*-ITD samples were more responsive toward gilteritinib and midostaurin, compared with *FLT3*-WT samples (Figure 1A and B).[3] We observed the most pronounced response of *FLT3*-ITD samples toward gilteritinib, exemplifying the known more potent and specific inhibition of FLT3 by gilteritinib compared with midostaurin, which has a broad inhibition profile (EC_{50} 12.9 versus 635.03 nM, https://proteomicsdb.org, Figure 1C).

Responses toward gilteritinib and midostaurin could not be fully explained by the presence of *FLT3*-ITD, with responses observed in *FLT3*-WT samples and relative resistance—exemplified by relatively high LC_{50} values—in *FLT3*-ITD samples (Figure 1D and E). To explore associations between response and phosphorylation, we compared phosphoproteomic profiles independent of *FLT3*-ITD status. We defined responsive and resistant samples based on the variation in LC_{50} values between patients: median LC_{50} for gilteritinib and the lowest and highest 25th percentile for midostaurin. For the pY phosphoproteome, the *FLT3*-ITD-independent response toward gilteritinib was associated with differential phosphorylation of 28 phosphosites ($P < 0.05$, Figure 1F and Supplemental Digital Table 3A, http://links.lww.com/HS/A167). Phosphosites with higher phosphorylation in gilteritinib-resistant samples included MAPK1-Y185, MAPK1-T187 (ERK2) and MAPK3-Y202 and MAPK3-T204 (ERK1), in concordance with other data on FLT3-TKI resistance, but not of FLT3 itself.[5,8–11] Posttranslational Modification Signature Enrichment Analysis (PTM-SEA, https://github.com/broadinstitute/ssGSEA2.0) indicated enrichment of EGFR1 (*P*

[1]Department of Hematology, Amsterdam UMC, Vrije Universiteit Amsterdam, Cancer Center Amsterdam, The Netherlands
[2]OncoProteomics Laboratory, Amsterdam UMC, Vrije Universiteit Amsterdam, Cancer Center Amsterdam, The Netherlands
[3]Medical Oncology, Amsterdam UMC, Vrije Universiteit Amsterdam, Cancer Center Amsterdam, The Netherlands
[4]Erasmus MC Cancer Institute, University Medical Center Rotterdam, Department of Hematology, Rotterdam, The Netherlands
[5]National Genetic Center, Muscat, Oman

The mass spectrometry proteomics data have been deposited to the ProteomeXchange Consortium via the PRIDE (http://www.ebi.ac.uk/pride) partner repository with the dataset identifier PXD024235.

Supplemental digital content is available for this article.

HemaSphere (2021) 5:7(e606).
http://dx.doi.org/10.1097/HS9.0000000000000606.
Received: 27 February 2021 / Accepted: 20 May 2021

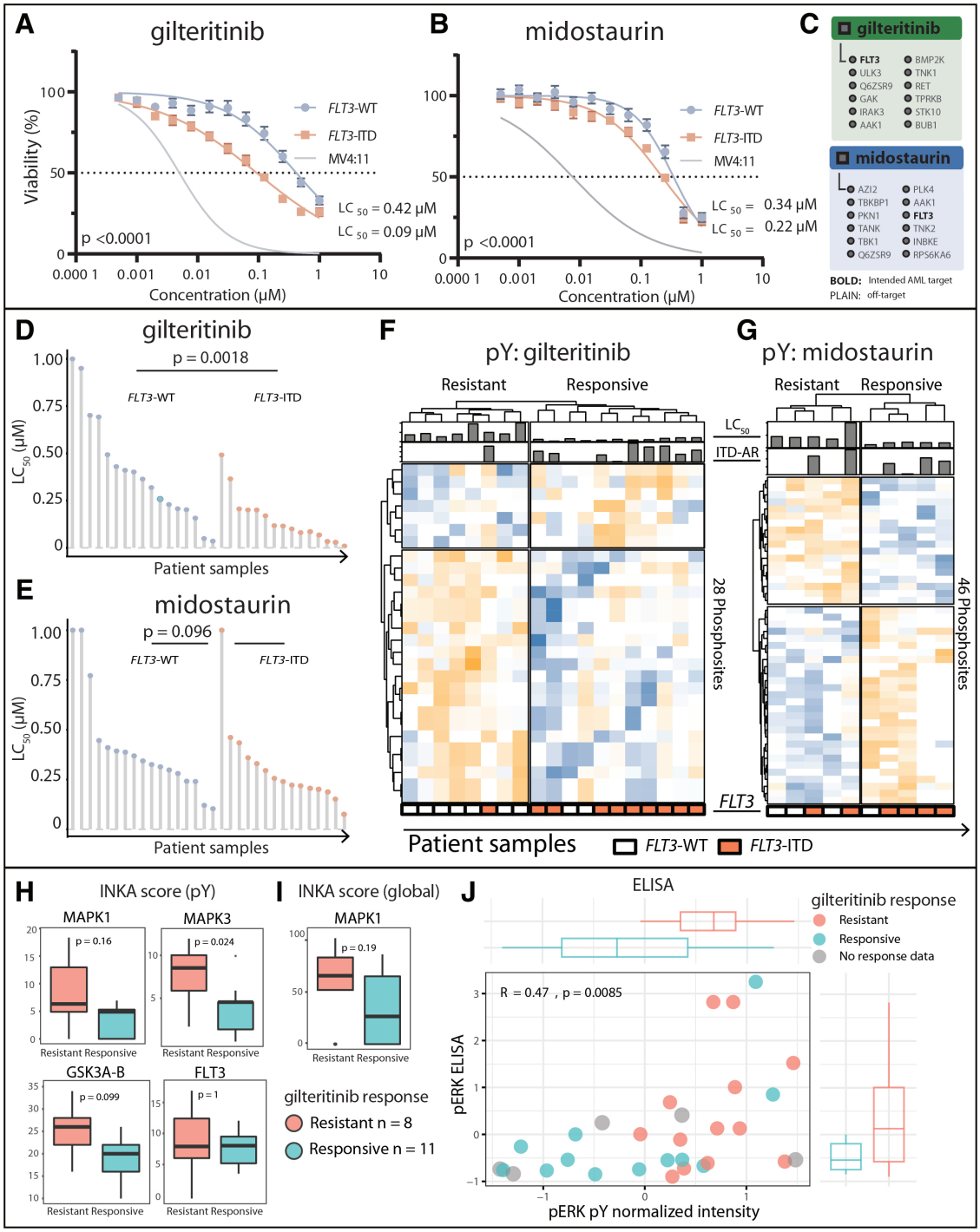

Figure 1. Response toward FLT3-TKIs and differential phosphorylation profiles and kinase activity scores associated with FLT3-TKI response. Ex vivo response of *FLT3*-WT and *FLT3*-ITD AML blasts toward (A) gilteritinib and (B) midostaurin. *P* values are calculated using least squares fit regression comparing *FLT3*-WT and *FLT3*-ITD samples. As workflow control, response of MV4:11, a homozygous *FLT3*-ITD AML cell line, is shown. (C) Protein target space of gilteritinib and midostaurin. The top 12 targets are shown, ranked on EC_{50}, which is the drug concentration at which half of the target is competed. Data are retrieved from https://proteomicsDB.org. Individual LC_{50} values as determined in liquid culture towards (D) gilteritinib and (E) midostaurin. The *P* value is determined using Wilcoxon rank-sum test. Additional samples for which no phosphoproteomics data was available are shown to illustrate the diversity in FLT3-TKI response. Phosphotyrosine phosphorylation profiles of significant ($P < 0.05$) differentially phosphorylated phosphosites between responsive and resistant primary AML samples towards (F) gilteritinib and (G) midostaurin. For heatmaps, Euclidean distance with complete linkage for rows and columns was applied. (H) INKA scores based on the pY analyses between gilteritinib responsive and resistant samples, based on median LC_{50}. (I) INKA score of MAPK1 based on the global phosphorylation analyses. *P* values are calculated by Wilcoxon rank-sum tests. (J) ELISA validation of pERK intensity as determined by pY phosphoproteomics, annotated with gilteritinib response. Correlation coefficient and *P* value were calculated using Pearson correlation. AML = acute myeloid leukemia; INKA = integrative inferred kinase activity; pY = phosphotyrosine.

< 0.05) and KIT ($P < 0.2$) pathway-associated phosphosites in resistant samples (Supplemental Digital Figure 3A, http://links.lww.com/HS/A167). Differential phosphorylation related to midostaurin response (Figure 1G and Supplemental Digital Table 3B, http://links.lww.com/HS/A167) was more diverse with 46 significant phosphosites, including high phosphorylation of

STAT6-Y531 in midostaurin responsive samples. Gene ontology analyses (g:Profiler, https://biit.cs.ut.ee/gprofiler/gost) revealed general processes related to kinase binding and transmembrane signaling. Ras-Raf-MEK-ERK-related phosphosites were absent among the identified differentially phosphorylated sites, although overexpression of *RGL4*—a regulator of this cascade—has been related to midostaurin response.[5] Comparison of global phosphoproteomic profiles between gilteritinib responsive and resistant samples did not yield any clear response-specific phosphorylation profiles (Supplemental Digital Figure 4A, http://links.lww.com/HS/A167). However, PTM-SEA revealed enrichment of phosphosites associated with KIT pathway activation ($P < 0.05$) and GSK3B activity ($P < 0.1$) in gilteritinib-resistant AML samples (Supplemental Digital Figure 3B, http://links.lww.com/HS/A167), which are independent from *FLT3*-ITD mutation status (Supplemental Digital Figure 3C and D, http://links.lww.com/HS/A167).

Integrative inferred kinase activity (INKA[12]) analysis of the pY phosphoproteome identified high activity of MAPK1, MAPK3, and GSK3A-B in gilteritinib-resistant samples, and confirmed that there was no differential activity of FLT3 (Figure 1H). Similarly, INKA analysis of the global phosphoproteome indicated higher activity of MAPK1 in gilteritinib-resistant samples (Figure 1I and Supplemental Digital Figure 5A–E, http://links.lww.com/HS/A167), suggesting that activation of FLT3-independent pathways may abrogate FLT3-inhibition and alternative pathways for survival may be targetable. Validation of pERK1/2 levels using ELISA suggests that high ERK phosphorylation is indeed associated with impaired response toward gilteritinib (Figure 1J). No significantly different INKA scores were identified in the midostaurin responsive versus resistant comparison.

To investigate which differential phosphorylated phosphosites between responsive and resistant samples were truly independent of *FLT3*-ITD status, we assessed phosphorylation differences between *FLT3*-WT and *FLT3*-ITD untreated de novo AML samples. As AML sample heterogeneity could hamper mutation-based analyses, we selected samples enriched with *FLT3*-ITD-positive blasts, on the basis of an allelic ratio of ≥ 0.5. In the pY data, 61 phosphosites were differentially ($P <$ 0.05) phosphorylated between *FLT3*-WT and *FLT3*-ITD AML. Phosphorylation of STAT5A-Y90 and LYN-Y265 was significantly higher in *FLT3*-ITD AML compared with *FLT3*-WT AML (Figure 2A–D and Supplemental Digital Table 3C, http://links.lww.com/HS/A167). STAT5A is a known downstream component of FLT3-ITD signaling.[13] While LYN may be activated by both FLT3-WT and FLT3-ITD, higher stochiometry of phosphorylation of FLT3-ITD may lead to higher binding of LYN.[1,14] Surprisingly, phosphorylation of FLT3 itself seemed independent of the presence of in-sample *FLT3*-ITD (Figure 2E and Supplemental Digital Figure 6, http://links.lww.com/HS/A167), indicating that not overall activity, but differential downstream activation distinguishes *FLT3*-WT from *FLT3*-ITD samples. Six phosphosites overlapped between differentially phosphorylated phosphosites of the mutation- and gilteritinib-response comparison (Figure 2F). Mutation-independent, response-specific differential phosphorylation (n = 22) included higher phosphorylation of MAPK1-T185, VIM-T63, STAT1-Y701, and Src-family kinases YES1, FYN, and SRC in gilteritinib-resistant samples. Phosphorylation of PTPN18-Y319 was low in resistant samples (Figure 2G). Global phosphorylation patterns were not clearly distinct between *FLT3*-WT and *FLT3*-ITD (Supplemental Digital Figure 4B and C, http://links.lww.com/HS/A167), although PTM-SEA identified known activation of mTOR and Pi3K-AKT signaling in *FLT3*-ITD samples (Supplemental Digital Figure 3D, http://links.lww.com/HS/A167).[15]

To further characterize *FLT3*-WT and *FLT3*-ITD AML on the protein expression level, we performed proteomics on 17 AML samples (9 *FLT3*-WT, 8 *FLT3*-ITD) with sufficient material for additional analyses. On the proteomic level, 4.092 unique proteins were identified, and 199 proteins were differentially ($P < 0.05$) expressed between *FLT3*-WT and *FLT3*-ITD samples (Supplemental Digital Figure 7A, http://links.lww.com/HS/A167 and Supplemental Digital Table 4, http://links.lww.com/HS/A167). Gene ontology analyses of proteins with a minimal fold change of 2 indicated that these proteins were primarily involved in leukocyte activation, oxidation-reduction processes, and protein activation cascades, including oncogenic MAPK signaling, stressing its important role in *FLT3*-ITD-biology (Supplemental Digital Figure 6B, http://links.lww.com/HS/A167). An integrated network with differentially expressed proteins and phosphorylated phosphosites for the *FLT3*-WT versus *FLT3*-ITD comparison—informed by the proteomic, global, and pY phosphoproteomic analyses—revealed relevant differential biology associated with *FLT3*-ITD-status, in particular cell activation (light green cluster), regulation of cell cycle (red cluster), and RNA splicing (light blue cluster) (Supplemental Digital Figure 8A, http://links.lww.com/HS/A167).

Impaired drug response associated with alternative pathway activation may be overcome by simultaneous blocking of those pathways. To replicate previously observed ex vivo therapeutic benefit of parallel MEK inhibition,[9] we assessed whether responses toward FLT3-TKIs would improve when treatment was combined with the MEK-inhibitor trametinib (Figure 2H). We only observed marginal decreases in LC_{50} for gilteritinib combined with fixed concentrations of trametinib (Figure 2I, K, L and Supplemental Digital Figure 9, http://links.lww.com/HS/A167). Surprisingly, we even observed an increase in LC_{50} towards both gilteritinib and midostaurin in several AML cases (Supplemental Digital Figures 9 and 10, http://links.lww.com/HS/A167), possibly explained by competitive antagonism or unexpected off-target effects. Using parallel increasing concentrations of gilteritinib or midostaurin and trametinib, synergy (exemplified by overall Bliss scores of > 10 [https://synergyfinder.fimm.fi/]) was only observed in a sample harboring an *NRAS* mutation (Figure 2J and Supplemental Digital Figures 9 and 10; http://links.lww.com/HS/A167), which may activate MEK-ERK signaling. Additionally, we explored the therapeutic effect of ulixertinib—a novel pan-ERK inhibitor. Combining gilteritinib with ulixertinib more efficiently enhanced response (Figure 2I, K, and L) than with trametinib. Combination of midostaurin with ulixertinib did not enhance responses (Supplemental Digital Figure 10, http://links.lww.com/HS/A167). Responses may be improved by optimizing concentrations and timing to prevent competitive antagonistic effects. Based on INKA ranking, AML patient-specific drug combinations could be explored[1] such as inhibition of KIT in AML2393: the differential phosphorylation of 2 KIT sites in the gilteritinib resistant samples (Figure 2F and Supplemental Digital Figure 8B, http://links.lww.com/HS/A167)—in tandem with the enrichment of KIT pathway components (Supplemental Digital Figure 3B, http://links.lww.com/HS/A167)—may in part explain our observations. KIT itself is a known driver of leukemogenesis and not inhibited by gilteritinib. KIT-Y936 site phosphorylation is a docking site for several signal transduction molecules, including GRB2 and CBL.[16] Binding of GRB2 to KIT can recruit GAB2 and may thereby mediate alternative activation of the MAPK signaling pathway and additionally activate the PI3K-Akt pathway in the gilteritinib-resistant samples.[17] Future studies may therefore explore combination treatment of gilteritinib with a KIT inhibitor in FLT3-TKI-resistant AML. Nevertheless, the marginal benefit of combining trametinib with FLT3-TKIs is discordant with previous reports[9] and warrants clarification to maximize the benefit of combinations with potentially toxic MEK inhibitors in clinical studies.

Our study has a few limitations. First, sample selection is biased toward highly proliferative AMLs allowing for ample (≥ 4.5 mg) protein extraction for in-depth pY phosphoproteomics

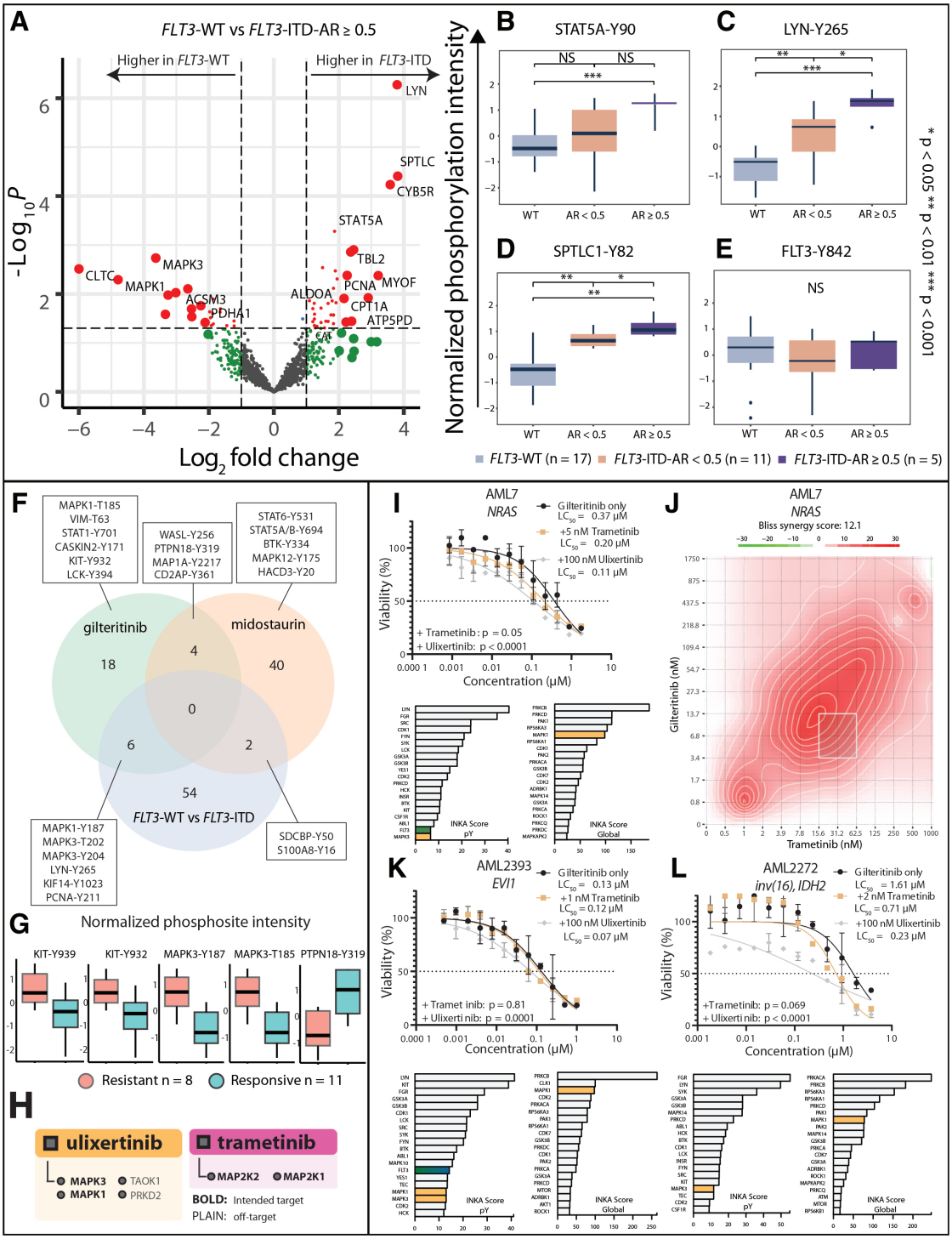

Figure 2. Phosphoproteomic characterization of FLT3-WT and FLT3-ITD AML and parallel treatment with FLT3- and MEK/ERK inhibitors of primary AML samples. (A) Volcanoplot of differentially ($P < 0.05$) phosphorylated proteins between *FLT3*-WT and *FLT3*-ITD AML samples and log2 fold changes. Specific phosphorylation according to *FLT3*-ITD status in AML samples of (B) STAT5-Y90; (C) LYN-Y265;244; (D) SPTLC1-Y82; and (E) FLT3-Y842. *P* values are calculated by Wilcoxon rank-sum tests. (F) Overlapping and unique differentially phosphorylated phosphosites from the pY phosphoproteomics comparisons of responsive and resistant samples towards gilteritinib and midostaurin, and *FLT3*-WT versus *FLT3*-ITD-AR > 0.5. (G) Normalized phosphosite intensities determined using pY-based phosphoproteomics of selected unique phosphosites between gilteritinib resistant and responsive AML samples. (H) Kinase target space of ulixertinib and trametinib. All targets are shown, ranked on EC_{50}, which is the drug concentration at which half of the target is competed. Data from https://proteomicsDB.org. (I, K, L) Combination treatment of AML samples with gilteritinib plus the LC_{10} of trametinib or ulixertinib and their individual INKA profiles from the pY and global phosphoproteomic analyses. (J) Combination treatment of AML7 with parallel increasing concentrations of gilteritinib and trametinib indicates synergism, exemplified by an overall Bliss synergy score of > 10. AML = acute myeloid leukemia; INKA = integrative inferred kinase activity; pY = phosphotyrosine.

analysis. Second, although we selected samples with high blast counts and enriched for mononuclear cells during pre-processing, samples also contained variable numbers of normal leukocytes. The small (< 10%) fraction of normal leukocytes present in the samples may have led to identification of some normal leukocyte biology associated phosphorylation events

in the (phospho)proteomics datasets. However, this should not affect the profiles associated with mutation status and drug response. Third, the observed associations are based on the ex vivo response of primary AMLs in liquid culture and require mechanistic validation using conditions mimicking the BM microenvironment,[18] which may impact the observed responses. As we compare relative resistance among samples cultured in identical culture conditions, our experiments still provide valuable information regarding response mechanisms. Nevertheless, clinical translation and validation of our findings is warranted: to further clarify response mechanisms on the phosphorylation level, future studies analyzing BM of patients treated with monotherapy FLT3-TKIs are required. Considering the current developments in AML treatment, however, most clinical studies will combine TKIs with other (targeted) agents or chemotherapy,[19] which should be taken into account in future research.

In conclusion, we present an in-depth clinical phosphoproteome dataset, characterizing *FLT3*-ITD AML and FLT3-TKI responses. We observed distinct phosphorylation signatures and protein expression profiles associated with response towards gilteritinib and midostaurin. Our ex vivo drug combination studies indicate that further exploration of the role of ERK and simultaneous blocking the MEK-ERK axis is warranted to maximize the potential benefit of treatment combinations aiming to improve responses to FLT3-TKIs. The identification of key proteins and phosphorylation events in *FLT3*-ITD-AML serve as a reference for future exploration of phosphoproteomic biomarkers associated with *FLT3*-ITD AML and FLT3-TKI response.

Disclosures

JJWMJ received research funding from Novartis and Bristol Myers Squibb; speaker fees from Incyte and Pfzer; advisory board honoraria from AbbVie, Incyte, Novartis, and Pfizer. He is the President of the Apps for Care and Science Foundation that develops the HematologyApp and which has received funding from Abbvie, Amgen, Astellas, Celgene/Bristol Myers Squibb, Daiichi-Sankyo, Incyte, Janssen, Jazz, Novartis, Sanofi Genzyme, Takeda, Roche, and Servier. All the other authors have no conflicts of interest to disclose.

Sources of funding

This study was partly funded by Stichting Egbers and Cancer Center Amsterdam (CCA2014-1-15 and CCA2012-5-08). Cancer Center Amsterdam and Netherlands Organization for Scientific Research (NWO Middelgroot, #91116017) are acknowledged for support of the mass spectrometry infrastructure.

References

1. van Alphen C, Cloos J, Beekhof R, et al. Phosphotyrosine-based phosphoproteomics for target identification and drug response prediction in AML cell lines. *Mol Cell Proteomics.* 2020;19:884–899.
2. Majothi S, Adams D, Loke J, et al. FLT3 inhibitors in acute myeloid leukaemia: assessment of clinical effectiveness, adverse events and future research-a systematic review and meta-analysis. *Syst Rev.* 2020;9:285.
3. Cucchi DGJ, Denys B, Kaspers GJL, et al. RNA-based FLT3-ITD allelic ratio is associated with outcome and ex vivo response to FLT3 inhibitors in pediatric AML. *Blood.* 2018;131:2485–2489.
4. Ambinder AJ, Levis M. Potential targeting of FLT3 acute myeloid leukemia. *Haematologica.* 2021;106:671–681.
5. Rosenberg MW, Watanabe-Smith K, Tyner JW, et al. Genomic markers of midostaurin drug sensitivity in FLT3 mutated and FLT3 wild-type acute myeloid leukemia patients. *Oncotarget.* 2020; 11:2807–2818.
6. Schaab C, Oppermann FS, Klammer M, et al. Global phosphoproteome analysis of human bone marrow reveals predictive phosphorylation markers for the treatment of acute myeloid leukemia with quizartinib. *Leukemia.* 2014;28:716–719.
7. van Alphen C, Cucchi DGJ, Cloos J, et al. The influence of delay in mononuclear cell isolation on acute myeloid leukemia phosphorylation profiles. *J Proteomics.* 2021;238:104134.
8. McMahon CM, Canaani J, Rea B, et al. Mechanisms of acquired resistance to Gilteritinib therapy in relapsed and refractory FLT3 -mutated acute myeloid leukemia. *Blood*. 2017;130(Suppl 1):295–295.
9. Morales ML, Arenas A, Ortiz-Ruiz A, et al. MEK inhibition enhances the response to tyrosine kinase inhibitors in acute myeloid leukemia. *Sci Rep.* 2019;9:18630.
10. Knapper S, Mills KI, Gilkes AF, et al. The effects of lestaurtinib (CEP701) and PKC412 on primary AML blasts: the induction of cytotoxicity varies with dependence on FLT3 signaling in both FLT3-mutated and wild-type cases. *Blood.* 2006;108:3494–3503.
11. Radomska HS, Bassères DS, Zheng R, et al. Block of C/EBP alpha function by phosphorylation in acute myeloid leukemia with FLT3 activating mutations. *J Exp Med.* 2006;203:371–381.
12. Beekhof R, van Alphen C, Henneman AA, et al. INKA, an integrative data analysis pipeline for phosphoproteomic inference of active kinases. *Mol Syst Biol.* 2019;15:e8250.
13. Choudhary C, Olsen JV, Brandts C, et al. Mislocalized activation of oncogenic RTKs switches downstream signaling outcomes. *Mol Cell.* 2009;36:326–339.
14. Okamoto M, Hayakawa F, Miyata Y, et al. Lyn is an important component of the signal transduction pathway specific to FLT3/ITD and can be a therapeutic target in the treatment of AML with FLT3/ITD. *Leukemia.* 2007;21:403–410.
15. Chen W, Drakos E, Grammatikakis I, et al. mTOR signaling is activated by FLT3 kinase and promotes survival of FLT3-mutated acute myeloid leukemia cells. *Mol Cancer.* 2010;9:292.
16. Masson K, Heiss E, Band H, et al. Direct binding of Cbl to Tyr568 and Tyr936 of the stem cell factor receptor/c-Kit is required for ligand-induced ubiquitination, internalization and degradation. *Biochem J.* 2006;399:59–67.
17. Wollberg P, Lennartsson J, Gottfridsson E, et al. The adapter protein APS associates with the multifunctional docking sites Tyr-568 and Tyr-936 in c-Kit. *Biochem J.* 2003;370:1033–1038.
18. Cucchi DGJ, Groen RWJ, Janssen JJWM, et al. Ex vivo cultures and drug testing of primary acute myeloid leukemia samples: current techniques and implications for experimental design and outcome. *Drug Resist Updat.* 2020;53:100730.
19. Cucchi DGJ, Polak TB, Ossenkoppele GJ, et al. Two decades of targeted therapies in acute myeloid leukemia. *Leukemia.* 2021;35:651–660.